Experiments to Systematically Evaluate the Role of Cohesion in Channel Initiation and Evolution

Nacere Mohamed Samassi[1,2], Fernando David Cúñez[1], and Rachel C. Glade[1,2]

[1]University of Rochester, Department of Earth and Environmental Sciences, 120 Trustee Rd, Rochester, NY, 14620. [2]University of Rochester, Department of Mechanical Engineering, 235 Hopeman Building, P.O. Box 270132, Rochester, NY, 14627-0132

[1]To whom correspondence should be addressed. Email: nsamassi@ur.rochester.edu

This manuscript is a non-peer reviewed preprint that has been submitted to EarthArXiv. The paper has been submitted to *GRL* for peer review. Updated versions will be uploaded as the paper (hopefully) traverses the peer review process.

Experiments to Systematically Evaluate the Role of Cohesion in Channel Initiation and Evolution

Nacere M. Samassi[1,2], Fernando D. Cúñez [1], and Rachel C. Glade[1,2]

[1]University of Rochester, Department of Earth and Environmental Sciences, 120 Trustee Rd, Rochester, NY, 14620.

[2]University of Rochester, Department of Mechanical Engineering, 235 Hopeman Building, P.O. Box 270132, Rochester, NY, 14627-0132

To whom correspondence should be addressed: Nacere Samassi (nsamassi@ur.rochester.edu) or Rachel Glade (rachel.glade@rochester.edu)

Key Points:

- Systematically changing cohesion in flume experiments leads to qualitative changes in erosional channel morphology and dynamics
- Increasing sediment cohesion leads to a transition from braided, to single thread, to gully-like channels with retreating headcuts
- Sediment velocities decrease with increasing cohesion, even with increasing discharge, illuminating cohesion effects on sediment transport

Abstract

Sediment and bank cohesion has long been known to exert a fundamental control on river morphology and dynamics. Here we present results from simplified laminar flume experiments to investigate how systematically increasing sediment cohesion affects erosional channel formation. Low cohesion leads to a subtle shift from highly mobile, braided-like to single-thread sinuous channels. At intermediate cohesion we observe an abrupt shift to a straight, narrow, gully-like channels with a retreating headcut despite little change in sediment transport rate. At higher cohesion, bedrock-like headcut retreat and sediment transport rate decreases due to highly stabilized banks and the dominance of aggregates. Our work demonstrates that even in simplified experiments, changes in cohesion alone can produce a wide range of channel forms strikingly similar to those observed at a range of scales and environmental conditions on Earth and other planets.

Plain Language Summary

We conducted laboratory experiments of river erosion with sticky, cohesive sediment and found that as cohesion increased, the river we made changed shape from braided channels to meandering channels, and to a single straight channel with a vertical cliff that retreated upstream through time. We analyzed the speed of the grains and found that higher cohesion slows down the movement of the sediments, which means the flow needs more force to start transporting the grains. We also saw that for the channel width, high cohesion produces narrower banks. Moreover, cohesion alters how the banks erode and how the grains clump together into aggregates. Our results show that conducting experiments with different amount of sediment cohesion provides fundamental insight into how rivers transition between different behaviors and forms, with implications for our understanding of channels on both Earth and other planets.

1 Introduction

Natural channels exhibit a variety of forms including braided rivers, single thread meandering rivers, gully-like channels with steep, retreating headcuts, and bedrock rivers. Previous work suggests that cohesion or substrate competence may be an important factor determining different river forms; for example, laboratory experiments have illustrated that bank cohesion is needed to transition from braided to single-thread channels (Parker 1978; Van Dijk et al., 2013; Tal & Paola, 2010; Brauderick et al., 2009; Peakall et al., 2007; Chadwick et al., 2025). While vegetation is a primary source of bank cohesion on Earth (Brauderick et al., 2009), other sources include abundant fine sediment, permafrost, and chemical cementation that may explain unvegetated single thread meandering channels found in both terrestrial modern (Santos et al., 2019; Ielpi et al., 2019a,b; Douglas et al., 2025) and paleo-environments (Ganti et al., 2019; Ielpi and Lapotre 2020; Valenza et al., 2023; Hasson et al., 2023; McMahon et al., 2024; Myrow et al., 2026), as well as on Mars (Matsubara et al., 2015; Lapotre et al., 2019). Further, cohesion may control channel width as it increases the critical shear stress τ_c of the banks (Kothyari and Jain, 2008; Rahimnejad and Ooi, 2016; Zhang and Yu, 2017; Lapotre et al., 2019; Dunne and Jerolmack

2020; Brunier-Coulin et al., 2020; Sharma et al., 2022; Chen et al., 2022), resulting in narrower channels in both gravel bed rivers (e.g., Andrews 1984; Huang and Warner 1995) and sand bed rivers (Kleinhans et al., 2015; Dunne and Jerolmack 2018, 2020). In a different setting, cohesion may also influence the formation of gullies and rills, rapidly eroding incipient channels that often form in response to disturbance (Bennett and Wells, 2019). Tucker et al., 2006 propose that in order to form gullies, tensile strength must be low enough to allow rapid erosion of sediment (e.g., de-vegetated agricultural lands (Prosser and Slade, 1994)), yet high enough to maintain steep banks and a retreating headcut characteristic of gullies (Kirkby and Bracken 2009). Cohesive soil is also needed to produce experimental gullies in the lab (e.g., Day et al., 2018; Bennett et al., 2000). Further, high substrate competence in bedrock rivers leads to similar mechanisms of headwall retreat (Izumi and Parker 1995; Lamb et al., 2006, 2009, 2014; Steelquist et al., 2023). While previous work suggests the importance of cohesion in fluvial erosion in different settings, to our knowledge cohesion controls on fluvial channel evolution have never been systematically evaluated experimentally.

Here we present the results of a series of simplified laminar flume experiments to determine how systematically increasing cohesion affects evolution of erosional channels on a loose to competent substrate continuum, thus enhancing our understanding of geomorphic systems in both natural and human altered landscapes.

2 Materials and Methods

We conducted flume experiments (Figure 1A) to explore how systematically increasing levels of cohesion alter channel dynamics, focusing on planform channel shape and headcut propagation. Inspired by Malarkey et al., 2015, we use xanthan gum (XG) to tune cohesion. XG, a polysaccharide secreted by the bacterium Xanthomonas campestris (Rosalam and England, 2006), is an appealing source of cohesion because 1) it is a type of extracellular polymeric substrate (EPS) produced by microbes that can be found in many natural landscapes (Jones et al., 2024) and has been used by humans to stabilize river banks (Smith et al., 2022) and increase cohesion of soils (Chen C., et al., 2019; Moghal et al., 2021), 2) is inexpensive, 3) is easy to mix with sediment, and 4) when wetted and subsequently dried, XG forms bridges between grains (Figure 1B) that maintain cohesive properties for a sufficient duration in our experiments (~1 hour) even when fully submerged (SI). In this context, we view cohesion as an additional stabilizing normal force between grains, resulting in a bulk tensile strength (e.g., Sharma et al., 2022). Following previous studies (e.g., Seizilles et al., 2013; Seizilles et al., 2014; Lajeunesse et al., 2010; Lobkovsky et al., 2008; Malverti et al., 2008), we conducted experiments in the laminar flow regime in order to simplify the experimental setup and minimize the role of turbulent noise, allowing better isolation of the role of cohesion in comparing different experimental runs. While this limits direct comparison of our experiments with natural alluvial rivers, our abstract, generalized experimental approach allows for a more controlled exploration of incisional channel formation in loose to competent substrate without attempting to reproduce a specific setting. To facilitate sediment transport in the laminar regime, we used angular, sand-sized plastic particles (MaxiBlast Wet-Blast®) with a density of 1500 kg/m^3 and particle diameters ranging from 0.25 to 0.42 mm (Figure 1B) that allowed us to maintain clear water and efficient sediment transport in our small setup (SI1).

Experiments were conducted in a 1 m long, 20cm wide flume at a slope of ~.002 with recirculating water, but no sediment recirculation or resupply. The base level condition was a 1 cm tall, 2 cm wide notch in the center of the flume outlet wall which promoted channelization and headcut retreat (Figure S1). A small notch at the inlet wall and a gently scraped initial straight depression allowed the channel to form in the middle of the flume. We prepared mixtures of 2300 g of plastic particles with varying concentrations of XG from 0 to 0.5% by weight, in line with preliminary measurements of EPS concentrations found in natural soils across the globe (Jones et al., 2024). Note that these conditions represent a cohesive substrate throughout the bed, not only the banks, in contrast to classic alluvial rivers. 1 L of water was added to each mixture, which was then evenly distributed across the flume bed at a depth of 2 cm. Because we were unable to quantify cohesion in our experiments, we report all results in terms of %XG rather than cohesion; however, observed cohesion clearly and substantially increased with each increment %XG. To ensure consistent compaction between experiments, we compressed the bed mixture using a 105 cm long, 17.2 cm thick wooden log, applied for 20 minutes. We allowed a drying period of about 24 hours before initiating the experiments to activate the XG bonds that produce cohesion between grains (Figure 2B). For each experiment, we began with a low flow rate to fill the initial shallow channel, then slowly increased the flow rate until we observed the beginning of sediment transport of individual grains. While precisely measuring Shields number was not possible, we estimate it ranged from 0.25-0.42 for the full range of grain size and flow conditions (SI1); these values are likely slightly above Shields stress, which has been shown to be ~0.125 in similar experiments using smaller plastic sediment (D = .09mm) in laminar water flow (Seizilles et al., 2014). As expected, discharges needed to move sediment increased with increasing %XG as cohesion increased τ_c (25 L/h for 0-0.2%XG, 40 L/h for 0.3%XG, and 55 L/h for 0.4-0.5%XG). For the most cohesive runs (0.4-0.5%XG), the increased discharge needed to move sediment led to shallow overland flow outside of the main channel (see Discussion). While some localized turbulence likely occurred in our experiments, we estimate that the maximum flow Reynolds number (Re) of the experiments ranged from ~60-800 depending on discharge, within the laminar range (Çengel and Cimbala, 2024); the particle Re ranged from ~8-32 (SI1). We also verified laminar flow by visualizing dye in the water. Before reaching the inlet, water from the pump passed through a layer of Styrofoam to regulate the flow and decrease turbulence. A layer of small gravel was placed at the outlet wall to minimize scour at the wall. The estimated maximum Froude number was subcritical in all experiments (~-.02 to 0.2; SI1).

Experiments were run until the channel either migrated to the sidewalls (low %XG runs) or stopped evolving entirely (high %XG runs, see Discussion) for a range of 20-140 minutes. We analyzed top-down experimental videos of the downstream-most 60cm of the flume captured at 60 fps to obtain sediment velocities using PIV (Particle Image Velocimetry) in PIVlab (Thielicke and Sonntag, 2021). Bank width and headcut locations were measured by hand in ImageJ (SI1). A second set of experiments showed that qualitative channel morphology changes due to cohesion are reproducible (SI2) (Church et al., 2020).

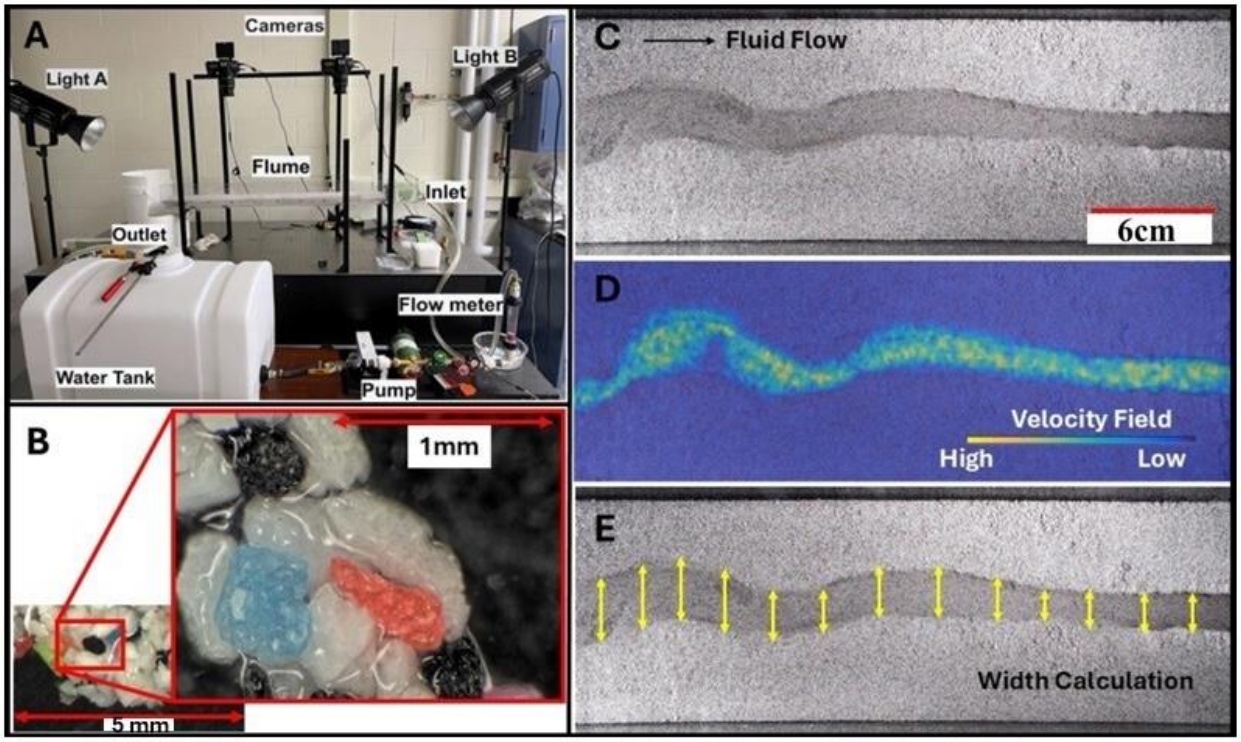

Figure 1: A) Experimental flume setup in the laboratory using a Global King Inc W15GR-15A pump. B) Microscope image showing xanthan gum bonds between sediment grains when wet and dry. Dry XG bonds strongly resemble water capillary bridges. C) Planform image of example channel formed for 0.1%XG D) Velocity field measured from PIV E) Illustration of hand-drawn extraction of bank widths.

3 Results

Our experiments show that with increasing cohesion, channels transition from a wide, highly mobile braided-like channel (0%XG) to a single thread sinuous channel (0.1%XG), to a narrower single thread straight gully-like channel with a rapidly retreating headcut, (0.2%XG), and finally to short, narrow, dendritic bedrock-like channels with headcuts (e.g., Vachtman and Laronne, 2013) that retreat more slowly as %XG increases (0.3-0.5%XG) (Figures 2,4). Videos show that grains move as bedload in all experiments, with rolling and hopping observed in the videos for all %XG. While some grains take long hops, likely due to the low specific gravity (1.5) of the plastic sediment, visible lateral grain motions due to collisions indicate that most grain maintain close contact with the bed throughout the experiment (Samassi 2026). Aggregates begin to form at 0.1%XG, with the onset of discrete bank collapse, and the size of aggregates gets larger with each incremental increase in %XG. However, some individual sediment grains are also still observed to move as bedload in all experimental runs. Using a minimum velocity cutoff of 0.2pixels/frame to remove immobile grains outside the main channel, we find that average sediment velocity magnitudes decrease by nearly an order of magnitude (from ~0.1 cm/s to ~0.01 cm/s) with increasing %XG (Figure 3). This occurs despite a twofold increase in discharge; indeed, mean grain velocity normalized by characteristic flow velocity (discharge/notch area) decreases with %XG (Figure 4C; non-normalized plot in Figure S4). While

all runs exhibit exponential-like grain velocity distributions, the 0-0.2%XG runs show a secondary peak of ~0.4 cm/s that disappears in higher %XG runs (Figure 3B). The variability of grain velocity also sytematically decreases with increasing %XG (Figure 4C). Qualitatively, the particle activity decreases substantially as cohesion is increased (Samassi 2026), likely leading to lower mean grain velocities as aggregates begin to dominate individual grain motions and the tail of the velocity distribution is progressively shortened (Figures 3B; 4C). We note that individual particle tracking at high frame rate would be required to observe accurate velocity distributions and means (e.g., Fathel et al., 2015); PIV-derived velocities are inherently averaged and therefore lower than individual grain velocities.

To explore bank widening and headcut retreat trends, we plot spatially averaged channel widths through time with standard deviation bars representing spatial variability in channel width (Figure 4A), along with headcut retreat distance through time (Figure 4B).

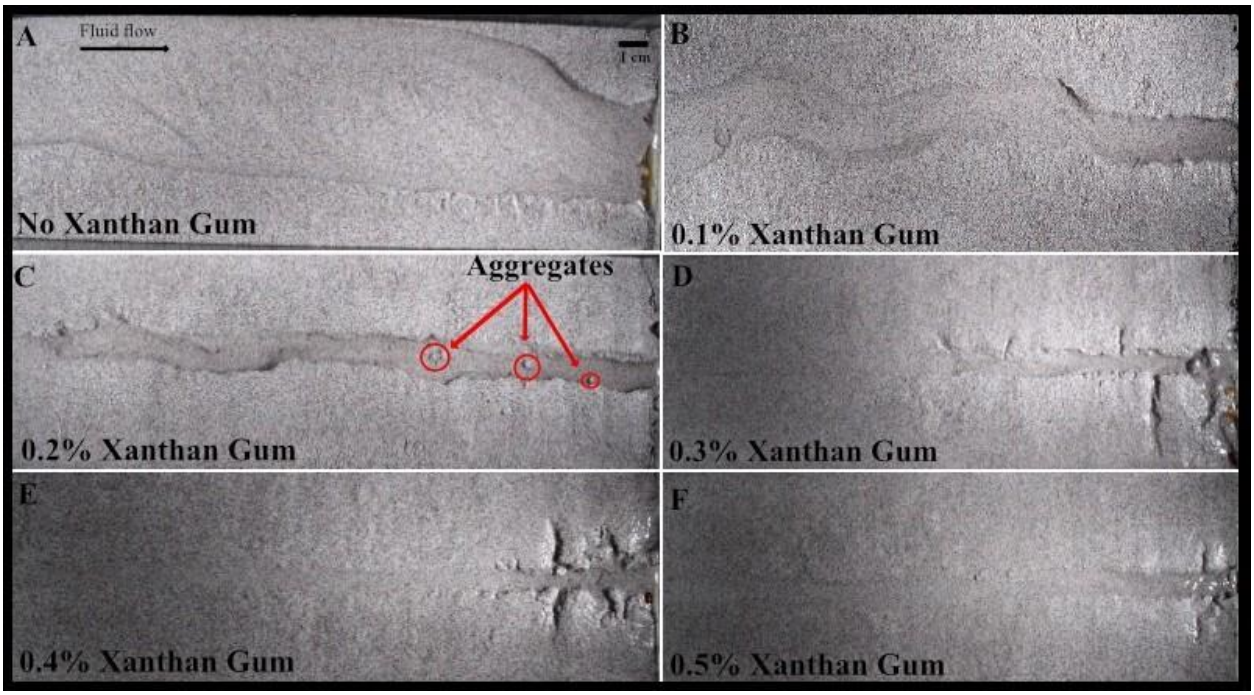

Figure 2: Representative images from each experiment with different %XG. Time of images: 0-0.1%XG (~minute 15); 0.2-0.3%XG (minute 40); 0.4-0.5%XG (minute 50).

At 0%XG, the highly mobile channel rapidly widens as soon as sediment motion begins and reaches a final width w_f of ~11 cm before migrating to the flume wall. The channel exhibits characteristics of braiding through time with multiple channel threads (Figure 2A). At 0.1%XG the overall pattern remains similar, with w_f ~10 cm and slightly lower spatial variability (Figure 4A). Qualitatively, the channel becomes more single-threaded as we observe signs of bank cohesion and the formation of small aggregates. At 0.2%XG, we observe an abrupt regime shift as w_f decreases dramatically to ~2.7 cm with much lower spatial varability. A defined headcut appears which retreats at a relatively constant rate of ~1cm/minute. These results suggest that the combination of moderate cohesion and persistent upstream migration places 0.2%XG in a

transitional regime where the channel is cohesive enough to maintain a retreating headcut but not cohesive enough to stop erosion completely.

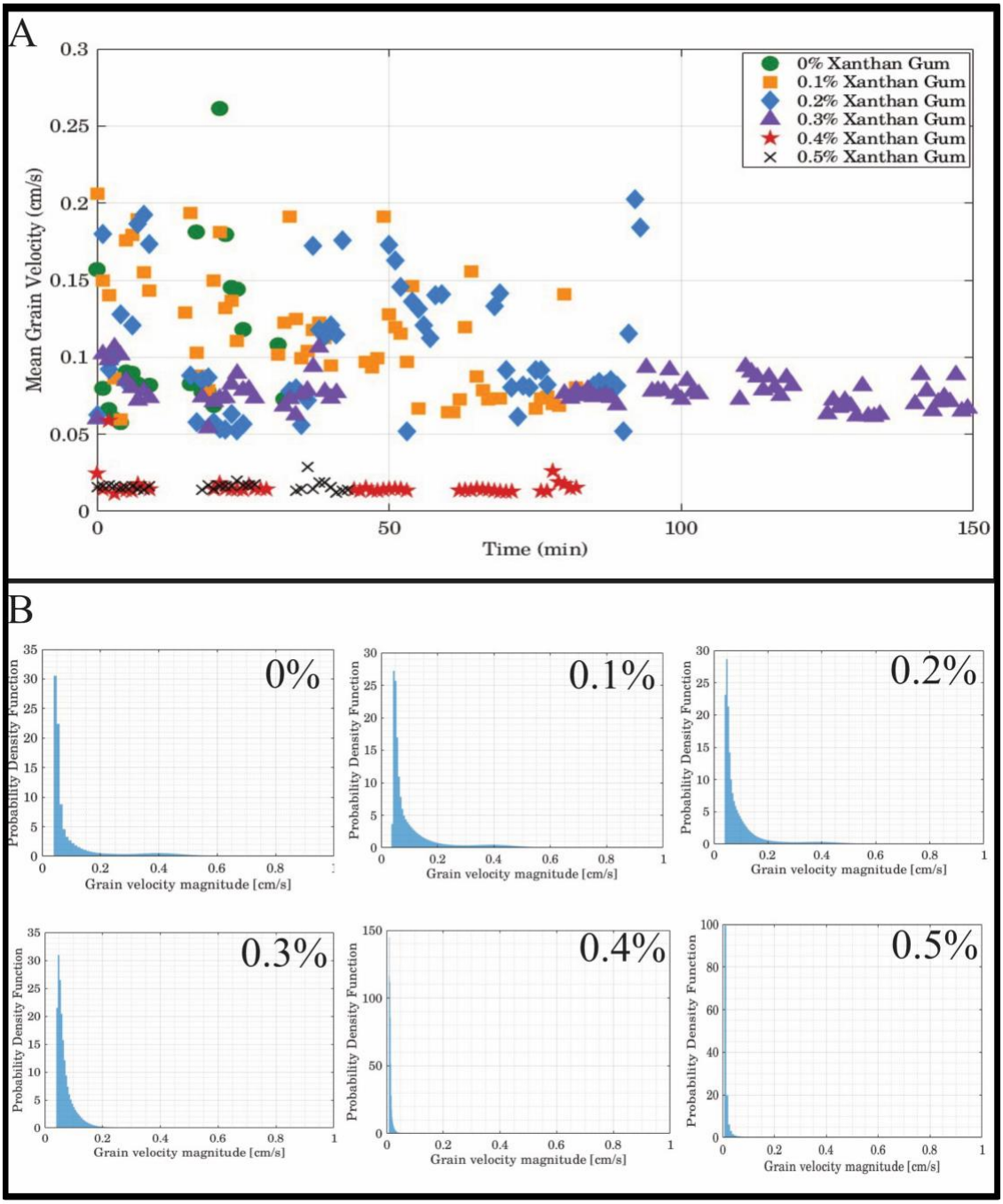

Figure 3: PIV results. A) Mean grain velocities through time for each %XG. SEM error bars are smaller than data points. B) PDFs of grain velocity magnitude for each %XG.

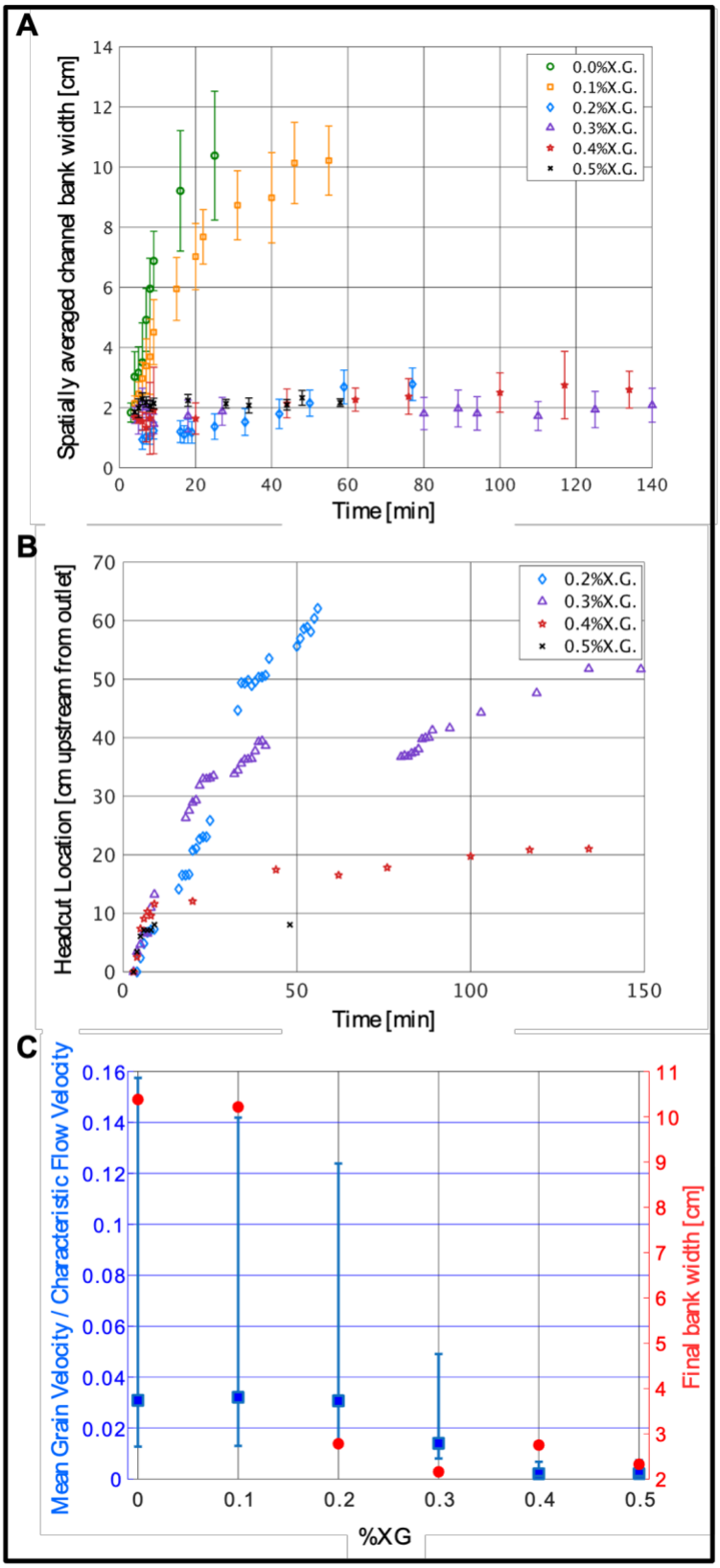
A
Spatially averaged channel bank width [cm]
Time [min]
0.0%X.G.
0.1%X.G.
0.2%X.G.
0.3%X.G.
0.4%X.G.
0.5%X.G.
B
Headcut Location [cm upstream from outlet]
Time [min]
0.2%X.G.
0.3%X.G.
0.4%X.G.
0.5%X.G.
C
Mean Grain Velocity / Characteristic Flow Velocity
Final bank width [cm]
%XG

Figure 4: Quantitative experimental results. A) Spatially averaged channel bank widths over time for different %XG with standard deviation. B) Headcut retreat distance over time for different %XG. The break in the data for 0.3% was due to a camera malfunction. C) Relationship between %XG, sediment velocity, and bank width. Left axis: PIV-derived mean sediment velocity magnitudes normalized by characteristic flow velocity (discharge/notch area) (blue squares) with 10^{th} and 90^{th} percentile error bars. Right axis: Final spatially averaged bank width (red dots). Discharges were 25 L/hr for 0-0.2%XG, 40 L/hr for 0.3%XG, and 55 L/hr for 0.4-0.5%XG.

At 0.3%XG, the channel continues to be narrow and straight, reaching a w_f of ~2 cm and a headcut retreat distance of 42.6 cm. At 0.4%XG and 0.5%XG, w_f is essentially constant at ~2.6 cm and ~2.2 cm, respectively, for the entire duration. The resulting morphology is similar to amphitheater-headed canyons found in bedrock channels (Lamb et al., 2014). Both concentrations produce very narrow channels with minimal headcut retreat distance: 18.95 cm for 0.4%XG and only 8.96 cm for 0.5%XG. While the initial headcut retreat rate was similar (~1 cm/min) for 0.2-0.5%XG, retreat rate slowed through time for 0.3-0.5%XG and became systematically slower as %XG increased (Figure 4B). We interpret that the cessation of headcut retreat results from a local decrease in channel slope at the headcut over time.

Overall, our results show that cohesion has a strong effect on channel morphology and sediment transport. We observe that channel widths decrease with increasing %XG, with low cohesion runs (0-0.1%XG) exhibiting channel widths nearly 5 times that of high cohesion runs (0.2-0.5%XG). Channel width exhibits more variability for low %XG, while higher %XG runs exhibit more narrow and stable channels likely due to the mechanical consequence of cohesive strength dominating over hydraulic shear (Figure 4A). Similarly, headcut retreat rates and sediment transport rate magnitude and variability decrease with increasing %XG. These decreases in width, headcut retreat and sediment transport occur *despite* increasing discharge needed to move higher cohesion grains, strengthening the observation that cohesion alone can profoundly alter channel behavior. Finally, as mean sediment transport rate does not decrease until 0.3%XG, the abrupt transition in channel width at 0.2%XG is largely decoupled from changes in sediment transport statistics.

4 Discussion

Our experiments demonstrate a profound effect of cohesion on channel morphology and evolution. One clear finding is that cohesion increases τ_c, as evidenced by the necessary increase in discharge for higher %XG runs. Further, as sediment velocity is generally thought to scale with excess fluid stress above critical (Meyer-Peter Müller 1948), our observed decrease in sediment velocity magnitude with %XG, even with increasing discharge, strongly points toward a cohesion-induced increase in τ_c that leads to channel narrowing—similar to the behavior observed in threshold alluvial streams (Phillips et al., 2022) especially with cohesive banks (e.g., Dunne and Jerolmack 2020), despite our erosional, supply limited setup. The role of cohesion in setting channel width is further demonstrated by the drastic decrease in channel width for increasing %XG, even in the face of increasing discharge (Figure 4C; SI3)—the inverse

of the expected width-discharge scaling seen in previous non-cohesive laminar flume experiments (Seizilles et al., 2013). Qualitative observations from experimental videos indicate two main mechanisms for the decrease in sediment velocity. First, XG bonds between individual grains modifies τ_c by adding a tensile strength that resists shear stress as seen in recent cohesive sediment experiments under an impinging jet (Brunier-Coulin et al., 2020; Sharma et al., 2022). Second, cohesion allows for the production of aggregates both from the bed and the banks, effectively increasing grain size and therefore decreasing the excess stress above threshold. While aggregates begin to form even at the lowest level of cohesion (0.1%XG), we observe an increase in aggregate size and dominance above individual grain transport as %XG increases. This may be reflected in the narrowing sediment velocity distributions and shortening tails of the PDFs (Figures 3B; 4C), as faster moving individual grains decrease and slower aggregates dominate the distributions. This decrease in sediment velocity variability may also explain the decrease in channel mobility and spatial variability of channel width with increasing cohesion. Finally, videos suggest that particle activity steadily decreases with %XG (Samassi 2026). As volumetric bedload flux is dominated more by particle activity than changes in mean sediment velocity (Roseberry et al., 2012), future work to explore the role of cohesion in altering particle activity may be fruitful.

While high levels of cohesion clearly alter sediment transport statistics, perhaps the most intriguing result of our experiment is the abrupt decrease in channel width at 0.2%XG without any change in discharge or mean sediment velocity magnitude (Figure 4C) and only a slight decrease in the 90^{th} percentile grain velocity (Figure 4C). In addition to the sudden narrowing of the channel, we observe that at 0.2%XG the banks have a threshold level of stability to maintain a near-vertical retreating headcut. This finding suggests that cohesion controls on channel morphology extend beyond simple changes in $\boldsymbol{\tau_c}$ or the formation of aggregates, likely due to a shift in bank erosion mechanism from shear driven grain-by-grain removal to strength-dependent bank collapse (e.g., Delenne et al., 2004). This observed threshold level of cohesion that drastically alters channel morphology without any change in sediment transport statistics is a key finding of this study. Further, 0.2%XG is the only case in which we observe steady retreat of the headcut through time; we posit that this intermediate state represents the “sweet spot” for gully initiation as envisioned by Tucker et al., 2006, in which the sediment is mobile enough to allow for efficient sediment transport yet cohesive enough to maintain steep headwalls, leading to the rapid retreat characteristic of destructive gully erosions in farmlands and other landscapes (Bennett and Wells, 2019).

At higher cohesion levels (0.3-0.5%XG), we observe the formation of secondary channels that develop alongside the main incised channel when the discharge exceeds what the narrow active channel can carry (Figure 2). First, this behavior suggests that larger discrete, cohesive bank failure events may allow secondary pathways to emerge during high flow conditions (Julian & Torres, 2006). Secondary channels may also develop due to variations in cohesion throughout the substrate mixture, where areas of lower cohesion create weak points that allow fluid shear forces to dislodge the grains. Another possible mechanism is the fact that the higher discharge needed to transport cohesive sediment encourages overland flow, allowing water to find more possible paths to follow. Because the main channel remained narrow due to cohesion, excess discharge gradually carved shallow secondary pathways on the floodplain. Therefore, while a thin sheet of water was present on the floodplain from the start, the

297 erosional secondary channels formed only after the onset of headcut retreat and sustained
298 morphodynamic adjustment. Further, XG may decrease the permeability of the sediment,
299 increasing the opportunity for overland flow (Zhang et al., 2024). While overland flow may just
300 be an artefact of our experimental setup, it is possible that a similar two-part effect occurs in
301 nature. First, in highly cohesive sediment, deeper overland flow may be needed to surpass the
302 threshold of motion for sediment and to initiate channels. Second, slow channel development
303 and headcut retreat may allow abundant water to find alternate flow paths at steep, newly
304 formed channel banks, producing secondary channels. Soil type and climate can influence both
305 cohesion and drainage density, ultimately affecting erosion processes (Moeini, et al., 2015;
306 Moragoda et al., 2022).
307 Our experiments have a number of limitations. For simplicity our experiments were
308 conducted in laminar flow, which previous work has shown can produce laboratory channels
309 with sediment transport mechanics and channel morphologies nearly identical to those found
310 in turbulent rivers (Malverti et al., 2008; Seizilles et al., 2013); however, we acknowledge that
311 turbulence must alter the details of both flow conditions and sediment transport in natural
312 rivers(Wilcock et al., 2003). Further, the presence of turbulence may be especially important in
313 cohesive channels by by introducing rapid, short timescale pressure and velocity fluctuations
314 that can momentarily exceed the cohesive strength of small aggregates or surface grains, and
315 can alter the mechanics of scour at retreating headcuts. Our simple experiments included
316 numerous measurement limitations; we could not record water or channel depth, which would
317 be needed to accurately estimate shear stress and channel geometry. Although we observed
318 morphology similar to braided and meandering streams, we emphasize that our exploratory
319 experiments with cohesion throughout the bed and no sediment supply explored the evolution
320 of erosional channels on a loose to competent substrate continuum, limiting their direct
321 applicability to natural alluvial streams. Our channels also do not reach an equilibrium state of
322 constant spatial width (e.g., Abramian et al., 2020) due to the boundary conditions (a narrow
323 notch at the outlet), lack of sediment supply and limited run time. Larger experiments could
324 examine turbulent cohesive channel formation, with a constant sediment feed, or with a thin
325 cohesive lid to better explore effects in alluvial channels, and could better quantify cohesion
326 with geotechnical testing. Grain scale numerical modelling should complement physical
327 experiments to better understand the mechanics of cohesive sediment transport (Vowinckel et
328 al., 2023).

329 **5 Conclusions**

330 Our results provide experimental evidence that systematically varying cohesion fundamentally
331 alters erosional channel initiation and evolution, producing a wide range of forms ranging from
332 wide, highly mobile braided-like channels to narrow gully-like channels with retreating
333 headcuts. Observations of channel narrowing with increasing cohesion along with PIV analysis
334 of grain velocities suggest that cohesion controls channel morphology both by altering τ_c and
335 allowing for qualitative differences in bank erosion processes, such as bank collapse and the
336 formation of aggregates. The abrupt shift in behavior at 0.2%XG with a constantly retreating
337 headcut without substantial changes in sediment transport statistics emphasizes the role of
338 bank stability and supports the idea of a goldilocks case in which cohesion is strong enough to
339 hold the bank of the headcut but too weak to stop ongoing bed erosion and retreat, as seen in

persistent gullies. Our experiments demonstrate that changes in cohesion alone can reproduce a wide array of qualitatively distinct fluvial channel forms and dynamics.

Acknowledgments

We thank Rory Cottrell, Hesam Askari, and Doug Kelley for their insightful conversations.

Open Research

Data and codes are available at Samassi (2026) and Glade and Samassi (2026).

Conflict of Interest Disclosure

The authors declare no conflicts of interest.

References

Abramian, A., Devauchelle, O., & Lajeunesse, E. (2020). Laboratory rivers adjust their shape to sediment transport. Physical Review E, 102(5), 053101. https://doi.org/10.1103/PhysRevE.102.053101

Andrews, E. D. (1984). Bed-material entrainment and hydraulic geometry of gravel-bed rivers in Colorado. *Geological Society of America Bulletin*, *95*(3), 371-378.

Bennett, S., Casalí, J., Robinson, K., & Kadavy, K. (2000). Characteristics of actively eroding ephemeral gullies in an experimental channel. Transactions of the ASAE, 43. https://doi.org/10.13031/2013.2745.

Bennett, S. J., & Wells, R. R. (2019). Gully erosion processes, disciplinary fragmentation, and technological innovation. *Earth surface processes and landforms*, *44*(1), 46-53.

365 Brauderick, C. A., Dietrich, W. E., Leverich, G. T., & Sklar, L. S. (2009). Experimental evidence for
366 the conditions necessary to sustain meandering in coarse-bedded rivers. *Proceedings of the*
367 *National Academy of Sciences*, *106*(40), 16936-16941.
368 Brunier-Coulin, F., Cuéllar, P., & Philippe, P. (2020). Generalized Shields criterion for weakly
369 cohesive granular materials. *Physical Review Fluids*, *5*(3), 034308.
370 Çengel, Y. A., & Cimbala, J. M. (2024). *Fluid mechanics: Fundamentals and applications*. McGraw
371 Hill.
372 Chadwick, Austin J., Evan Greenberg, and Vamsi Ganti (2025). Single-and multithread rivers
373 originate from (im)balance between lateral erosion and accretion. *Science* 389, 146-150.
374 Chen, C., Wu, L., Perdjon, M., Huang, X., & Peng, Y. (2019). The drying effect on xanthan gum
375 biopolymer treated sandy soil shear strength. *Construction and Building Materials*, *197*, 271-
376 279.
377 Chen, D., Zheng, J., Zhang, C., Guan, D., Li, Y., & Huang, H. (2022). Threshold of surface erosion
378 of cohesive sediments. *Frontiers in Marine Science*, *9*, 847985.
379 Church, M., Dudill, A., Venditti, J. G., & Frey, P. (2020). Are results in geomorphology
380 reproducible?. *Journal of Geophysical Research: Earth Surface*, *125*(8), e2020JF005553.
381 Day, S. S., Gran, K. B., & Paola, C. (2018). Impacts of changing hydrology on permanent gully
382 growth: experimental results. *Hydrology and Earth System Sciences*, *22*(6), 3261-3273.
383 Delenne, J. Y., El Youssoufi, M. S., Cherblanc, F., & Bénet, J. C. (2004). Mechanical behaviour and
384 failure of cohesive granular materials. *International Journal for Numerical and Analytical*
385 *Methods in Geomechanics*, *28*(15), 1577-1594.

386 Douglas, Madison M., Kimberly Litwin Miller, and Michael P. Lamb (2025). "Mud cohesion
387 governs unvegetated meander migration rates and deposit architecture." Geological Society of
388 America Bulletin 137.1-2: 522-540.
389 Dunne, K. B., & Jerolmack, D. J. (2018). Evidence of, and a proposed explanation for, bimodal
390 transport states in alluvial rivers. *Earth Surface Dynamics*, *6*(3), 583-594.
391 Dunne, K. B. J., & Jerolmack, D. J. (2020). What sets river width?. Science Advances, 6,
392 eabc1505. https://doi.org/10.1126/sciadv.abc1505
393 Fathel, S. L., Furbish, D. J., & Schmeeckle, M. W. (2015). Experimental evidence of statistical
394 ensemble behavior in bed load sediment transport. *Journal of Geophysical Research: Earth*
395 *Surface*, *120*(11), 2298-2317.
396 Ganti, V., Whittaker, A. C., Lamb, M. P., & Fischer, W. W. (2019). Low-gradient, single-threaded
397 rivers prior to greening of the continents. *Proceedings of the National Academy of Sciences*,
398 *116*(24), 11652-11657.
399 Hasson, M., Marvin, M. C., Gunn, A., Ielpi, A., & Lapôtre, M. G. (2023). A depositional model for
400 meandering rivers without land plants. *Sedimentology*, *70*(7), 2272-2301.
401 Huang, H. Q., & Warner, R. F. (1995). The multivariate controls of hydraulic geometry: a causal
402 investigation in terms of boundary shear distribution. *Earth Surface Processes and Landforms*,
403 *20*(2), 115-130.
404 Ielpi, A. (2019). Morphodynamics of meandering streams devoid of plant life: Amargosa River,
405 Death Valley, California. *Bulletin*, *131*(5-6), 782-802.
406 Ielpi, A., & Lapôtre, M. G. (2019). Barren meandering streams in the modern Toiyabe Basin of
407 Nevada, USA, and their relevance to the study of the pre-vegetation rock record. *Journal of*

Sedimentary Research, *89*(5), 399-415.

Ielpi, A., & Lapôtre, M. G. (2020). A tenfold slowdown in river meander migration driven by plant life. *Nature Geoscience*, *13*(1), 82-86.

Izumi, N., & Parker, G. (1995). Inception of channelization and drainage basin formation: upstream-driven theory. *Journal of Fluid Mechanics*, *283*, 341-363..

Jones, N. A. (2024, November). Do Microbes Shape Landscapes? Investigating Clays, Crusts, and Extracellular Polymeric Substances (EPS) in Mars Analog Environments. In *ASA, CSSA, SSSA International Annual Meeting*. ASA-CSSA-SSSA.

Julian, J. P., & Torres, R. (2006). Hydraulic erosion of cohesive riverbanks. *Geomorphology*, *76*(1-2), 193-206.

Kirkby, M. J., & Bracken, L. J. (2009). Gully processes and gully dynamics. *Earth Surface Processes and Landforms: The Journal of the British Geomorphological Research Group*, *34*(14), 1841-1851.

Kleinhans, M. G., Van Scheltinga, R. T., Van Der Vegt, M., & Markies, H. (2015). Turning the tide: Growth and dynamics of a tidal basin and inlet in experiments. *Journal of Geophysical Research: Earth Surface*, *120*(1), 95-119.

Kothyari, U. C., & Jain, R. K. (2008). Influence of cohesion on the incipient motion condition of sediment mixtures. *Water resources research*, *44*(4).

Lajeunesse, E., Malverti, L., Lancien, P., Armstrong, L., Metivier, F., Coleman, S., ... & Parker, G. (2010). Fluvial and submarine morphodynamics of laminar and near-laminar flows: A synthesis. *Sedimentology*, *57*(1), 1-26.

Lamb, M. P., Howard, A. D., Johnson, J., Whipple, K. X., Dietrich, W. E., & Perron, J. T. (2006). Can springs cut canyons into rock?. *Journal of Geophysical Research: Planets*, *111*(E7).

Lamb, M. P., & Dietrich, W. E. (2009). The persistence of waterfalls in fractured rock. *Geological Society of America Bulletin*, *121*(7-8), 1123-1134.

Lamb, M. P., Mackey, B. H., & Farley, K. A. (2014). Amphitheater-headed canyons formed by megaflooding at Malad Gorge, Idaho. *Proceedings of the National Academy of Sciences*, *111*(1), 57-62.

Lapôtre, M. G., Ielpi, A., Lamb, M. P., Williams, R. M., & Knoll, A. H. (2019). Model for the formation of single-thread rivers in barren landscapes and implications for pre-Silurian and Martian fluvial deposits. *Journal of Geophysical Research: Earth Surface*, *124*(12), 2757-2777.

Lobkovsky, A. E., Orpe, A. V., Molloy, R., Kudrolli, A., & Rothman, D. H. (2008). Erosion of a granular bed driven by laminar fluid flow. *Journal of Fluid Mechanics*, *605*, 47-58.

Malarkey, J., Baas, J. H., Hope, J. A., Aspden, R. J., Parsons, D. R., Peakall, J., ... & Thorne, P. D. (2015). The pervasive role of biological cohesion in bedform development. *Nature communications*, *6*(1), 6257.

Malverti, L., Lajeunesse, E., & Métivier, F. (2008). Small is beautiful: Upscaling from microscale laminar to natural turbulent rivers. *Journal of Geophysical Research: Earth Surface*, *113*(F4).

Matsubara, Y., Howard, A. D., Burr, D. M., Williams, R. M., Dietrich, W. E., & Moore, J. M. (2015). River meandering on Earth and Mars: A comparative study of Aeolis Dorsa meanders, Mars and possible terrestrial analogs of the Usuktuk River, AK, and the Quinn River, NV. *Geomorphology*, *240*, 102-120.

McMahon, W. J., Herron, S. T., Craig, J. A., & Davies, N. S. (2024). Mud retention in hydrologically closed basins promoted pre-vegetation meandering: evidence from the Neoproterozoic Diabaig Formation, Scotland.

Meyer, P. E., & Muller, R. (1984, January). Formulas for bed-load transport. PROCEEDING MEETING IAHR.

Moeini, A., Zarandi, N. K., Pazira, E., & Badiollahi, Y. (2015). The relationship between drainage density and soil erosion rate: a study of five watersheds in Ardebil Province, Iran. *WIT Trans Ecol Environ*, *1*, 129-138.

Moghal, A. A. B., & Vydehi, K. V. (2021). State-of-the-art review on efficacy of xanthan gum and guar gum inclusion on the engineering behavior of soils. *Innovative Infrastructure Solutions*, *6*(2), 108.

Moragoda, N., Kumar, M., & Cohen, S. (2022). Representing the role of soil moisture on erosion resistance in sediment models: Challenges and opportunities. *Earth-Science Reviews*, *229*, 104032.

Myrow, P. M., Gaines, R. R., & Lamb, M. P. (2026). Low sinuosity meandering rivers before vascular plants: Cambrian Tapeats Formation, Arizona, USA. *Geological Society of America Bulletin*, *138*(1-2), 809-822.

Parker, G. (1978) Self-formed straight rivers with equilibrium banks and mobile bed. part 2. The gravel river. J. Fluid Mech. 89, 127–146

Peakall, J., Ashworth, P. J., & Best, J. L. (2007). Meander-bend evolution, alluvial architecture, and the role of cohesion in sinuous river channels: a flume study. *Journal of Sedimentary Research*, *77*(3), 197-212.

Phillips, C.B., Masteller, C.C., Slater, L.J. *et al.* Threshold constraints on the size, shape and stability of alluvial rivers. *Nat Rev Earth Environ* 3, 406–419 (2022).

Prosser, I. P., & Slade, C. J. (1994). Gully formation and the role of valley-floor vegetation, southeastern Australia. *Geology*, *22*(12), 1127-1130.

Rahimnejad, R., & Ooi, P. S. (2016). Factors affecting critical shear stress of scour of cohesive soil beds. *Transportation Research Record*, *2578*(1), 72-80.

Rosalam, S., & England, R. (2006). Review of xanthan gum production from unmodified starches by Xanthomonas comprestris sp. Enzyme and Microbial Technology, 39(2), 197- 207. https://doi.org/10.1016/j.enzmictec.2005.10.019

Roseberry, J. C., Schmeeckle, M. W., & Furbish, D. J. (2012). A probabilistic description of the bed load sediment flux: 2. Particle activity and motions. *Journal of Geophysical Research: Earth Surface*, *117*(F3).

Samassi, N. (2026). Cohesion Experiment Videos [Dataset]. https://figshare.com/s/65117fb242d5af1d3612

Samassi, N. & Glade, R. (2026). Supporting data for Samassi et al., "Experiments to Systematically Evaluate the Role of Cohesion in Channel Initiation and Evolution" [Dataset, Software]. Zenodo. https://doi.org/10.5281/zenodo.20076995

Santos, M. G., Hartley, A. J., Mountney, N. P., Peakall, J., Owen, A., Merino, E. R., & Assine, M. L. (2019). Meandering rivers in modern desert basins: Implications for channel planform controls and prevegetation rivers. *Sedimentary Geology*, *385*, 1-14.

Seizilles, G., Lajeunesse, E., Devauchelle, O., & Bak, M. (2014). Cross-stream diffusion in bedload transport. *Physics of Fluids*, *26*(1).

494 Seizilles, G., Devauchelle, O., Lajeunesse, E., & Métivier, F. (2013). Width of laminar laboratory
495 rivers. *Physical Review E—Statistical, Nonlinear, and Soft Matter Physics*, *87*(5), 052204.
496 Sharma, R., Gong, M., Azadi, S., Gans, A., Gondret, P., & Sauret, A. (2022). Erosion of cohesive
497 grains by an impinging turbulent jet. Physical Review Fluids, 7.
498 https://doi.org/10.1103/PhysRevFluids.7.074303
499 Smith, D. J., Snead, M., & Thompson, T. M. (2022). Soil amended with organic matter increases
500 fluvial erosion resistance of cohesive streambank soil. *Journal of Geophysical Research:*
501 *Biogeosciences*, *127*(6), e2021JG006723.
502 Steelquist, A. T., Lapôtre, M. G. A., & Hilley, G. E. (2023). Drainage initiation, expansion, and
503 channel-head arrest in heterogenous bedrock landscapes of the Colorado Plateau. *Bulletin*,
504 *135*(5-6), 1344-1358.
505 Tal, M., & Paola, C. (2010). Effects of vegetation on channel morphodynamics: results and
506 insights from laboratory experiments. *Earth Surface Processes and Landforms*, *35*(9), 1014-
507 1028.
508 Thielicke, W., & Sonntag, R. (2021). Particle Image Velocimetry for MATLAB: Accuracy and
509 enhanced algorithms in PIVlab.
510 Tucker, G. E., Arnold, L., Bras, R. L., Flores, H., Istanbulluoglu, E., & Solyom, P. (2006).
511 Headwater channel dynamics in semiarid rangelands, Colorado high plains, USA. *Geological*
512 *Society of America Bulletin*, *118*(7-8), 959-974.
513 Vachtman, D., & Laronne, J. B. (2013). Hydraulic geometry of cohesive channels undergoing
514 base level drop. *Geomorphology*, *197*, 76-84.

Valenza, J. M., Ganti, V., Whittaker, A. C., & Lamb, M. P. (2023). Pre-Vegetation, Single-Thread Rivers Sustained by Cohesive, Fine-Grained Bank Sediments: Mesoproterozoic Stoer Group, NW Scotland. *Geophysical Research Letters*, *50*(14), e2023GL104379.

Van Dijk, W. M., Teske, R., Van de Lageweg, W. I., & Kleinhans, M. G. (2013). Effects of vegetation distribution on experimental river channel dynamics. *Water Resources Research*, *49*(11), 7558-7574.

Vowinckel, B., Zhao, K., Zhu, R., & Meiburg, E. (2023). Investigating cohesive sediment dynamics in open waters via grain-resolved simulations. *Flow*, *3*, E24.

Wilcock, P. R., & Crowe, J. C. (2003). Surface-based transport model for mixed-size sediment. *Journal of hydraulic engineering*, *129*(2), 120-128.

Zhang, M., & Yu, G. (2017). Critical conditions of incipient motion of cohesive sediments. *Water Resources Research*, *53*(9), 7798-7815.

Zhang, J., Cheng, Y., Liu, J., Jiang, T., & Sun, D. A. (2024). Permeability of xanthan gum-improved silty soil and its prediction model. *Bulletin of Engineering Geology and the Environment*, *83*(4), 130.

538